Research Article

Shreen El-Sapa* and Munirah Aali Alotaibi

Migration of two rigid spheres translating within an infinite couple stress fluid under the impact of magnetic field

https://doi.org/10.1515/phys-2024-0085
received July 07, 2024; accepted August 19, 2024

Abstract: In this study, we examine the movement of two hard spheres aligned in a straight line within an incompressible couple stress fluid under the impact of the magnetic field. Both objects have distinct shapes and move along an axis connecting their centers with varying velocities. As a first step, an incompressible analytical analysis is performed on a fluid with couple stress properties around an axially symmetric particle. Using the superposition principle, a general solution is developed for couple stress fluid flows over two moving objects. In order to achieve the boundary conditions, the boundary collocation strategy is applied to the surfaces of the two spheres. A set of tables and graphs illustrates numerical estimates of the dimensionless drag forces acting on two spherical objects. In addition, a drop in Hartmann number or an increase in couple stress viscosity will increase the dimensionless drag force on each spherical particle.

Keywords: magnetic field, couple stress fluid, drag force, interaction, collocation method

1 Introduction

A wide variety of physical, geophysical, and industrial domains use the motion of conducting fluids in an electromagnetic field. Magnetohydrodynamics (MHD) effects can control fluid travel past solid objects in these real-world contexts. The classical problem of Hartmann flow has numerous essential applications in many fields, including MHD pumps and power generators, heating, polymer technology, aerodynamics, the petroleum industry, crude oil purification, and heat exchanger design. The study of transporting fluids past solid surfaces of diverse shapes has also emerged due to recent breakthroughs in rocketry and spacecraft. Bearman and Wadcock [1] discussed the interaction between the flows around two circular cylinders when they are shifted in a plane perpendicular to the free stream and brought near together. A study was carried out by Yutaka *et al.* [2] to investigate the fluid dynamic interaction between two spheres to gather fundamental knowledge about the flow of two-phase fluids, particularly in the dense phase. Faltas *et al.* [3] proposed a solution for the interaction between two spherical particles revolving in a micropolar fluid. Shehadeh and Ashmawy [4] examined the continuous linear movement of two aligned solid spheres in an incompressible couple stress fluid.

Several investigations have sought to determine the influence of an applied magnetic field on the movement of an electrically conductive fluid around a spherical or cylindrical object. MHD is an area of science that focuses on comprehending the behavior of fluids when exposed to a magnetic field's influence. The presence of MHD in a fluid flow has the potential to manage flow separation, optimize heat transfer, and alter fluid flow velocity. Chandrasekhar [5] has made observations about how a magnetic field affects rotating cylinders' viscous flow consistency. Davis *et al.* [6] demonstrated the hydrodynamic modification of a rigid elastic sphere that is submerged in a viscous fluid and moving into another sphere or a solid surface. An inviscid conducting fluid with a strong magnetic field was the subject of Stewartson's [7] examination of a fully conducting spherical in steady motion. When the sphere moves in the same direction as the field, the streamlines outside the sphere appear as straight lines. However, when the sphere moves perpendicular to the field, the streamlines exhibit abrupt twists. Saad [8] conducted a study on the influence of a magnetic field on the flow around a porous sphere and cylinders enclosed by a cell. Srivastava [9] investigated the

* **Corresponding author: Shreen El-Sapa,** Department of Mathematical Sciences, College of Sciences, Princess Nourah bint Abdulrahman University, P.O. Box 84428, Riyadh 11671, Saudi Arabia, e-mail: seelsapa@pnu.edu.sa
Munirah Aali Alotaibi: Department of Mathematical Sciences, College of Sciences, Princess Nourah bint Abdulrahman University, P.O. Box 84428, Riyadh 11671, Saudi Arabia, e-mail: maalotaiby@pnu.edu.sa

implications of MHD regarding the hydrodynamic porosity of a permeable membrane consisting of spherical particles. Madasu and Bucha [10] examined the MHD impact of the movement of fluid through a partially permeable spherical particle and derived a clear expression for drag. Also, they analyzed the flow of MHD past a cylindrical shill using Brinkman's model for the problem of parallel flow [11]. El-Sapa [12] investigated the impact of slip and magnetic field on the motion of a solid sphere that is moving perpendicular to an infinite rigid wall in an unbounded viscous fluid. El-Sapa and Alsudais [13] investigated, on the assumption of Stock's conditions, the effects of the magnetic field on two stiff spheres with varying slip conditions on their surfaces in a permeable media. El-Sapa and Faltas [14] studied the continuous and almost consistent straight motion of two spherical particles immersed in an infinite magnetomicropolar fluid. Several recent scholarly articles have concentrated on the subject of how a magnetic field affects the flow of fluid [15–19].

MHD and couple stress fluid are distinct ideas that can be integrated to investigate the flow characteristics of electrically conductive fluids with certain attributes. Through the examination of MHD in the context of couple stress fluid flow, scientists acquire a more profound comprehension of the intricacies of fluid dynamics in scenarios encompassing: fluid with microstructure that can conduct electricity, magnetic fields employed for regulating the flow of a substance, enhancement of filtration, and lubrication procedures. Nadeem and Akram [20] performed a research investigation on the movement of fluid with qualities of couple stress in a channel that is not symmetrical, while considering the impact of the magnetic field that is created. The solutions for the equations of magnetic field and momentum have been accurately calculated, under the assumption of the long wavelengths and a low, but non-zero Reynolds number. Hassan [21] investigated the examination of a hydromagnetic fluid flow that undergoes a chemical reaction, specifically focusing on couple stress fluids. The flow occurs through a channel that is filled with porous particles. Srinivasacharaya and Rao [22] provided numerical solutions for the constant flow of MHD blood *via* a branched artery with a slight narrowing in the main channel, including heat transfer and assuming blood to be fluid with couple stress. Ali *et al*. [23] conducted a study on the MHD flow and heat transfer of a couple stress fluid across an oscillating stretching band in a porous medium with a heat source/sink. Alotaibi and El-Sapa [24] investigated the translation motion of a rigid sphere enclosed by a concentric sphere filled with a MHD fluid that exhibits coupling stress. The study considered the effects of slippage and the Hatmann number. The investigation of couple stress fluids is seen crucial for comprehending various physical phenomena, particularly in the field of biomedicine.

Drag force refers to the opposition encountered by an object as it travels through a fluid, which be either a liquid or a gas. This opposing force acts in the direction opposite to an object's motion. The amount of the drag force is influenced by various parameters, such as the velocity of the object, the dimensions and configuration of the item, the density, and the consistency of the fluid. Hoffmann *et al.* [25] analyzed the opposition encountered by a spherical object in micropolar fluids taking into account non-uniform boundary conditions for the microrotation vector. Ashmawy [26] derived a comprehensive equation for the drag experienced by a sphere immersed in a slow and time-varying flow of a micropolar fluid. Shu and Lee [27] developed fundamental solutions for micropolar fluids generated by a singular point force and a singular point pair. Later on, the aforementioned solutions were used to calculate the drag force applied to a solid sphere moving in a micropolar flow with a low Reynolds number. Sherief *et al.* [28] formulated a mathematical equation to determine the drag force exerted on a symmetrical object that is in motion at a consistent speed within a microstrech fluid.

Approximately 50 years ago, Gluchman *et al*. [29] created a novel method for treating multiple particles that are immersed in an infinitely slow viscous flow. This approach is a numerical method commonly known as the Frontier collocation technique. Their theoretically predicted drag results show a high level of agreement with the experimental evidence. The fundamental concept behind employing the collection approach to address the flow issue at a low Reynolds number is to compute the velocity field generated by every coordinate boundary. This is achieved through the methodical arrangement of fundamental solutions that are suitable for the particular constant orthogonal surface. The coefficients in the fundamental solutions are determined by the specified boundary conditions. The series, which represents the solution, is shortened and the boundary criteria are only applied at certain locations referred to as collocation points. Several studies have made use of this approach [30–34]. Conversely, several numerical techniques exist for examining this interplay between the objects, and also show the interactions and chemical applications, which are elucidated through previous studies [35–41].

The purpose of this study is to demonstrate how two rigid spheres traveling rectilinearly on a shared axis interact with each other during axial movement. The spheres are subjected to the impact of a magnetic field in an incompressible fluid with couple stress properties. The surfaces of the two spheres are exposed to boundary conditions where there is no couple tension and no sliding. An incompressible

object moving steadily in an infinite series may represent the semi-analytical solution for the couple stress fluid *via* an axis-symmetric object. The general solution for the stable motion of a fluid with couple stress, as it flows past two spheres that are moving in a straight line along their centers, is constructed by combining the obtained solution with the superposition principle. Two spherical coordinate systems are employed, each with its origin located in the center of a solid sphere. The collocation approach is utilized to satisfy the prescribed border constraints on the spherical surfaces. The dimensionless drag force acting based on the solid spheres is calculated and sketched. Analyzing numerical results will be accomplished by graphing the results.

2 MHD couple stress fluid equations

Therefore, couple stresses primarily affect the creation of a length-dependent impact, which is nonexistent from the standard model of non-polar fluid dynamics. Couple stress fluid hypothesis was introduced by Stokes [42] in 1984, building over the well-known Navier–Stokes theories. The current investigation is based on the assumptions that [43] and [44] examine: (a) the fluid is incompressible because of its homogeneous, isotropic density, (b) since the Lorentz force is only magnetic, uneven polarization and electric charge are inconsequential, (c) the movement is creeping because magnetic Reynold's number $R = Uav\sigma$ and Reynold's number $R = \frac{Ua}{\nu}$ are deemed to display an appropriate level of humility. A term representing inertia is disregarded, (d) the couple stress is ignored, as is the body force operating across the flow direction, (e) there is no external electric field, and (f) this analysis is isothermal. Moreover, previous studies [43–45] provide the MHD couple stress fluid equations of motion as.

$$\nabla\cdot\vec{q} = 0, \tag{2.1}$$

$$\begin{aligned}&\mu\nabla\wedge\nabla\wedge\vec{q} + \eta\nabla\wedge\nabla\wedge\nabla\wedge\nabla\wedge\vec{q}\\&\quad= -\nabla p + \mu_e^2\sigma(\vec{q}\wedge\vec{H})\wedge\vec{H},\end{aligned} \tag{2.2}$$

where ∇ is the spherical partial differential operator, $\vec{q}$ is the volume-averaged velocity, p is the pore average pressure, μ represents the viscosity of the fluid, η is the first couple stress viscosity coefficient, η' is the second couple stress viscosity coefficient. If the couple stress coefficient η is taken zero, then the equation of motion (2.2) reduces to the classical Navier–Stokes's equation. The basis of classical electromagnetism is made up of the Lorentz force law and an ensemble of related partial differential equations known as the Maxwell–Heaviside equations are given as

$$\left.\begin{aligned}&\mathrm{div}\vec{E} = 0, \quad \mathrm{div}\vec{H} = 0,\\&\mathrm{curl}\vec{E} = -\frac{\partial\vec{B}}{\partial t}, \quad \mathrm{curl}\vec{H} = \vec{J} + \frac{\partial\vec{D}}{\partial t},\end{aligned}\right\} \tag{2.3}$$

where $\vec{B} = \mu_e\vec{H}, \vec{D} = \varepsilon\vec{E}, \vec{B}\wedge\vec{J} = \sigma\vec{B}\wedge(\vec{E} + \vec{q}\wedge\vec{B})$, the magnetic field vector is $\vec{H}$, the electric field vector $\vec{E}$, the fluid pressure is p, the magnetic permeation is μ_e, μ is the viscosity coefficient, the electric conduction is σ. η, and η' are the couple stress viscosities. Additionally, $\vec{J}$, $\vec{B}$, and $\vec{D}$ represent the current density, magnetic induction, and electric displacement vectors, accordingly. Whenever $\eta = 0$ (2.2) is provided the Newtonian fluids by Prasad and Sarkar [43].

The constitutive relations listed in the following describe couple stress fluids:

$$\tau_{ij} = -p\delta_{ij} + 2\mu d_{ij} - \frac{1}{2}\varepsilon_{ijk}m_{sk,a}, \tag{2.4}$$

$$m_{ij} = m\delta_{ij} + 4(\eta'\omega_{i,j} + \eta\omega_{j,i}), \tag{2.5}$$

where τ_{ij} and m_{ij} are the stress and couple stress tensors respectively, the alternating tensor is ε_{ijk}, and the Kronecker delta is δ_{ij}. Furthermore, the deformation stress tensor is $d_{ij} = \frac{1}{2}(q_{i,j} + q_{j,i})$, and the spin function is $\omega_i = \frac{1}{2}\varepsilon_{ijk}q_{k,j}$.

These inequalities are satisfied by the viscosity coefficients in the couple stress fluid calculations:

$$0 \le \mu, 0 \le \eta, \eta' - \eta \le 0, 0 \le 3\lambda + 2\mu. \tag{2.6}$$

Consequently, the earlier provided mathematical equations have been assigned the subsequent non-dimensional characteristics:

$$\begin{aligned}&\vec{q}^* = \frac{\vec{q}}{U}, \vec{\omega}^* = \frac{a\vec{\omega}}{U}, p^* = \frac{ap}{\mu U}, \nabla^* = a_\nabla, \tau_{rr}^* = \frac{a\tau_{rr}}{\mu U},\\&\alpha^2 = \frac{a^2}{\kappa},\\&\xi = \sqrt{\frac{a^2\mu}{\eta}}, \vec{H}^* = \frac{\vec{H}}{H_0}, R_H = \sqrt{\frac{\mu_e^2a^2H_0^2\sigma}{\mu}}.\end{aligned} \tag{2.7}$$

After substituting Eq. (2.7) into (2.2), disregarding the asterisks for simplicity, and using the slowing flow from the earlier assumptions, we obtain [43]

$$\begin{aligned}&\nabla p + \frac{1}{\xi^2}\nabla\wedge\nabla\wedge\nabla\wedge\nabla\wedge\vec{q} + \nabla\wedge\nabla\wedge\vec{q}\\&\quad - R_H^2(\vec{q}\wedge\vec{H})\wedge\vec{H} = 0.\end{aligned} \tag{2.8}$$

Using Lorentz's force, the equation for a non-polar fluid (2.8) is an updated version of the Stokes equation, where

R_H represents the Hartmann number, if ξ approaches infinity. If $R_H = 0$, the Stokes approach to modeling the behavior of a fluid with couple stress.

The function stream ψ can be utilized for describing the velocity features:

$$q_r(r,\theta) = \frac{-1}{r^2\sin\theta}\frac{\partial\psi}{\partial\theta}, \quad q_\theta(r,\theta) = \frac{1}{r\sin\theta}\frac{\partial\psi}{\partial r}. \tag{2.9}$$

Additionally, the vorticity vector can be defined as follows:

$$\vec{\omega} = \frac{1}{2}\nabla \wedge \vec{q} = \frac{E^2\psi}{2r\sin\theta}\vec{e}_\phi. \tag{2.10}$$

Then, with the help of Eq. (2.9) the continuity Eq. (2.1) is immediately achieved, which reduces to:

$$0 = -\frac{\partial p}{\partial r} - \frac{1}{r^2\sin\theta}\frac{\partial}{\partial\theta}E^2\psi + \frac{1}{\xi^2}\frac{1}{r^2\sin\theta}\frac{\partial}{\partial\theta}E^2(E^2\psi) + R_H^2\frac{1}{r^2\sin\theta}\frac{\partial\psi}{\partial\theta}, \tag{2.11}$$

$$0 = -\frac{1}{r}\frac{\partial p}{\partial\theta} + \frac{1}{r\sin\theta}\frac{\partial}{\partial r}E^2\psi - \frac{1}{\xi^2}\frac{1}{r\sin\theta}\frac{\partial}{\partial r}E^2(E^2\psi) - R_H^2\frac{1}{r\sin\theta}\frac{\partial\psi}{\partial r}, \tag{2.12}$$

where $E^2 = \frac{\partial^2}{\partial r^2} + \frac{1-\zeta^2}{r^2}\frac{\partial^2}{\partial\xi^2}$, $\zeta = \cos\theta$. One can derive the subsequent six-order partial differential formula by removing pressure from Eqs (2.11) and (2.12)

$$E^2(E^2 - k_1^2)(E^2 - k_2^2)\psi = 0, \tag{2.13}$$

where the roots of (3.6) are obtained by

$$\left.\begin{aligned} &k_1^2 + k_2^2 = \xi^2,\ k_1^2k_2^2 = \xi^2R_H^2 \\ &k_i = \sqrt{\frac{\xi^2 \pm \xi\sqrt{\xi^2 - 4R_H^2}}{2}}, \quad i = 1,2 \end{aligned}\right\}. \tag{2.14}$$

3 MHD couple stress fluid over a moving rigid sphere

Under the assumption that fluid motion is axisymmetric, meaning that every value acts independently of ϕ, (r,θ,ϕ) represents the spherical polar structure. The rigid sphere of radius a is translated at a uniform velocity U through unbounded MHD couple stress fluid. Furthermore, the stream function, the velocities, and the vorticity components are established by the following:

$$\psi(r,\theta) = \sum_{n=2}^{\infty}\Big[A_nr^{-n+1} + B_nr^{\frac{1}{2}}K_{n-\frac{1}{2}}(k_1r) + C_nr^{\frac{1}{2}}K_{n-\frac{1}{2}}(k_2r)\Big]G_n(\zeta), \tag{3.1}$$

$$q_r = -\sum_{n=2}^{\infty}\Big[A_nr^{-n-1} + B_nr^{\frac{-3}{2}}K_{n-\frac{1}{2}}(k_1r) + C_nr^{\frac{-3}{2}}K_{n-\frac{1}{2}}(k_2r)\Big]P_{n-1}(\zeta), \tag{3.2}$$

$$q_\theta = \sum_{n=2}^{\infty}\Big[(1-n)A_nr^{-n-1} + B_nr^{\frac{-3}{2}}(nK_{n-\frac{1}{2}}(k_1r) - k_1rK_{n+\frac{1}{2}}(k_1r)) + C_nr^{\frac{-3}{2}}(nK_{n-\frac{1}{2}}(k_2r) - k_2rK_{n+\frac{1}{2}}(k_2r))\Big]\frac{G_n(\zeta)}{\sqrt{1-\zeta^2}}. \tag{3.3}$$

From Eq. (3.3), the vorticity component is

$$\omega_\phi = \frac{1}{2}\sum_{n=2}^{\infty}r^{\frac{-1}{2}}\Big[B_nk_1^2K_{n-\frac{1}{2}}(k_1r) + C_nk_2^2K_{n-\frac{1}{2}}(k_2r)\Big]\frac{G_n(\zeta)}{\sqrt{1-\zeta^2}}. \tag{3.4}$$

The set of constants A_n, B_n, and C_n must be computed using the constraints on the boundary that have been applied to the boundary region.

The formula can be used to calculate the force of the drag produced by an incompressible medium [34]. The flow of a couple stress fluid is characterized by infinite stretching along the axisymmetric object as it moves in the same direction.

$$F_z = 8\pi\mu\lim_{r\to\infty}\frac{\psi}{r\sin^2\theta}. \tag{3.5}$$

The following formula is obtained by combining (3.1) with the drag formula (3.5):

$$F_z = 2\mu\pi R_H^2Ua\left(\frac{2}{3} + A_2\right). \tag{3.6}$$

As is well known, $F_\infty = -6\pi\mu Ua$ represents the force of drag operating on a rigid sphere traveling in a uniform incompressible viscous flow of fluid [26]. When we compare our findings to the special situation of viscous fluid, this latter formula will be helpful.

4 Interaction of two rigid spheres within magneto couple stress fluid

This section analyzes the uniform-state translating motion of an incompressible couple stress fluid past two inline hard spheres. Two hard objects having radii of a_j, $j = 1, 2$, and uniform velocities of U_j, $j = 1, 2$, respectively, translate along a common axis that connects their centers to produce the fluid motion. As seen in Figure 1, the two spherical objects are situated outside of one another. It is believed

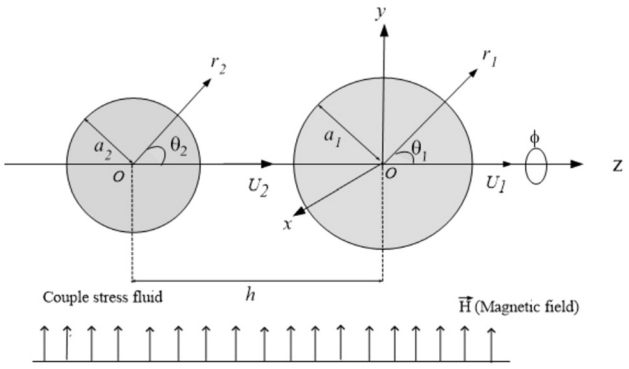

Figure 1: Sketch of two spheres in a magneto-couple stress fluid.

that the fluid is at rest at a great distance from the two spheres. Dual spherical coordinate systems, (r_1, θ_1, ϕ) and (r_2, θ_2, ϕ), having origins at the centers of spheres a_1 and a_2, respectively, are conveniently considered. While the boundaries are axisymmetric, the angle ϕ has no bearing on any of the flow field functions. Furthermore, the following relations tie the two coordinate systems (r_1, θ_1) and (r_2, θ_2) to one another:

$$\left.\begin{aligned} r_1^2 &= r_2^2 + h^2 - 2r_2 h\cos\theta_2, \\ r_2^2 &= r_1^2 + h^2 + 2r_1 h\cos\theta_1. \end{aligned}\right\} \tag{4.1}$$

The Stokesian flow presumption will be used, assuming that the velocities are modest. In these conditions, all hydrodynamic functions are not dependent on ϕ and the flow is axially symmetric. In the event when the second item is absent, take $\vec{q}^{\,j}$ to represent the velocity vector of the couple stress fluid caused by the existence of the spherical particles a_j. We select $\tau_{r\theta}^{(j)}$, $\vec{q}^{(j)}$, $\vec{\omega}^{(j)}$, and $m_{r\phi}^{(j)}$ in the following manner:

$$\left.\begin{aligned} \vec{q}^{(j)}(r_j, \theta_j) &= q_r^{(1)}(r_1, \theta_1) + q_r^{(2)}(r_2, \theta_2), \\ m_{r_j\phi}^{(j)}(r_j, \theta_j) &= m_{r_1\phi}^{(1)}(r_1, \theta_1) + m_{r_2\phi}^{(2)}(r_2, \theta_2). \end{aligned}\right\} \tag{4.2}$$

The separation of variables technique is the conventional approach to solve a sixth-order linear partial differential Eq. (2.13):

$$\begin{aligned} \psi(r, \theta) = \sum_{j=1}^{2}\sum_{n=2}^{\infty}\Bigg[& A_n^{(j)} r_j^{-n+1} + B_n^{(j)} r_j^{\frac{1}{2}} K_{n-\frac{1}{2}}(k_1 r_j) \\ & + C_n^{(j)} r_j^{\frac{1}{2}} K_{n-\frac{1}{2}}(k_2 r_j)\Bigg] G_n(\zeta_j). \end{aligned} \tag{4.3}$$

The second-kind modified Bessel equations of degree n are defined by $K_n(.)$, accordingly. The constants $A_n^{(j)}, C_n^{(j)}, B_n^{(j)}, E_n^{(j)}, D_n^{(j)}, F_n^{(j)}, j = 1, 2$ can be derived from the boundary conditions (4.1). The components of velocity are

$$\begin{aligned} q_r = -\sum_{j=1}^{2}\sum_{n=2}^{\infty}\Bigg[& A_n^{(j)} r_j^{-n-1} + B_n^{(j)} r_j^{\frac{-3}{2}} K_{n-\frac{1}{2}}(k_1 r_j) \\ & + C_n^{(j)} r_j^{\frac{-3}{2}} K_{n-\frac{1}{2}}(k_2 r_j)\Bigg] P_{n-1}(\zeta_j). \end{aligned} \tag{4.4}$$

$$\begin{aligned} q_\theta = \sum_{j=1}^{2}\sum_{n=2}^{\infty}\Bigg[& (1-n) A_n^{(j)} r_j^{-n-1} + B_n^{(j)} r_j^{\frac{-3}{2}} (nK_{n-\frac{1}{2}}(k_1 r_j) \\ & - k_1 r_j K_{n+\frac{1}{2}}(k_1 r_j)) + C_n^{(j)} r_j^{\frac{-3}{2}} (nK_{n-\frac{1}{2}}(k_2 r_j) \\ & - k_2 r_j K_{n+\frac{1}{2}}(k_2 r_j))\Bigg] \frac{G_n(\zeta_j)}{\sqrt{1-\zeta_j^2}}. \end{aligned} \tag{4.5}$$

From Eq. (3.3), the vorticity and couple stress components are

$$\begin{aligned} \omega_\phi = \frac{1}{2}\sum_{j=1}^{2}\sum_{n=2}^{\infty} r_j^{\frac{-1}{2}}\Bigg[& B_n^{(j)} k_1^2 K_{n-\frac{1}{2}}(k_1 r_j) \\ & + C_n^{(j)} k_2^2 K_{n-\frac{1}{2}}(k_2 r_j)\Bigg] \frac{G_n(\zeta_j)}{\sqrt{1-\zeta_j^2}}. \end{aligned} \tag{4.6}$$

$$\begin{aligned} m_{r\phi}(r, \theta) = \sum_{j=1}^{2}\sum_{n=2}^{\infty} r_j^{\frac{-3}{2}}\Bigg[& B_n^{(j)} k_1^2 \Bigg(((n-1)\xi^{-2} - \xi'^{-2}) K_{n-\frac{1}{2}} \\ & - \xi^{-2} k_1 r_j K_{n+\frac{1}{2}}(k_1 r_j)\Bigg) \\ & + C_n^{(j)} k_2^2 \Bigg(((n-1)\xi^{-2} - \xi'^{-2}) K_{n-\frac{1}{2}} \\ & - \xi^{-2} k_2 r_j K_{n+\frac{1}{2}}(k_2 r_j)\Bigg)\Bigg] \frac{G_n(\zeta_j)}{\sqrt{1-\zeta_j^2}}. \end{aligned} \tag{4.7}$$

For Eq. (2.14), we should have the six boundary conditions to describe the problem fully. The assumptions of Stokes [42] state that the physical interactions on the outer edge are equal to force dispersion mainly because there are no couple stresses at the spherical object interface. The two spheres translate with different velocities $U_j, j = 1, 2$ such that the kinematic and dynamic boundary conditions on the two surfaces of the solid objects $r_j = a_j, j = 1, 2$ are

$$\begin{aligned} q_r(r_j, \theta_j) &= U_j\cos\theta_j, \\ q_\theta(r_j, \theta_j) &= -U_j\sin\theta_j, \\ m_{r_j\phi}(r_j, \theta_j) &= 0. \end{aligned} \tag{4.8}$$

Inputting in the left-hand side of the boundary constraints (4.5)–(4.13) for $r_j = a_j, j = 1, 2$, we obtain the equations of velocity and couple stress provided by (4.4), (4.5), and (4.7):

$$\sum_{n=2}^{\infty}\Bigg[A_n^{(1)}a_1^{-n-1}+B_n^{(1)}a_1^{\frac{-3}{2}}K_{n-\frac{1}{2}}(k_1a_1)+C_n^{(1)}a_1^{\frac{-3}{2}}K_{n-\frac{1}{2}}(k_2a_1)\Bigg]P_{n-1}(\zeta_1)+\sum_{n=2}^{\infty}\Bigg[A_n^{(2)}r_2^{-n-1}+B_n^{(2)}r_2^{\frac{-3}{2}}K_{n-\frac{1}{2}}(k_1r_2)+C_n^{(j)}r_2^{\frac{-3}{2}}K_{n-\frac{1}{2}}(k_2r_2)\Bigg]\Bigg|_{r_1=a_1}\times P_{n-1}(\zeta_2)=-\zeta_1,\tag{4.9}$$

$$\sum_{n=2}^{\infty}\Bigg[A_n^{(1)}r_1^{-n-1}+B_n^{(1)}r_1^{\frac{-3}{2}}K_{n-\frac{1}{2}}(k_1r_1)+C_n^{(1)}r_1^{\frac{-3}{2}}K_{n-\frac{1}{2}}(k_2r_1)\Bigg]\Bigg|_{r_2=a_2}P_{n-1}(\zeta_1)+\sum_{n=2}^{\infty}\Bigg[A_n^{(2)}a_2^{-n-1}+B_n^{(2)}a_2^{\frac{-3}{2}}K_{n-\frac{1}{2}}(k_1a_2)+C_n^{(j)}a_2^{\frac{-3}{2}}K_{n-\frac{1}{2}}(k_2a_2)\Bigg]P_{n-1}(\zeta_2)=-\bar{U}\zeta_2,\tag{4.10}$$

$$\sum_{n=2}^{\infty}\Bigg[(1-n)A_n^{(1)}a_1^{-n-1}+B_n^{(1)}a_1^{\frac{-3}{2}}\Bigg(nK_{n-\frac{1}{2}}(k_1a_1)-k_1a_1K_{n+\frac{1}{2}}(k_1a_1)\Bigg)+C_n^{(1)}a_1^{\frac{-3}{2}}\Bigg(nK_{n-\frac{1}{2}}(k_2a_1)-k_2a_1K_{n+\frac{1}{2}}(k_2a_1)\Bigg)\Bigg]\frac{G_n(\zeta_1)}{\sqrt{1-\zeta_1^2}},+\sum_{n=2}^{\infty}\Bigg[(1-n)A_n^{(2)}r_2^{-n-1}+B_n^{(2)}r_2^{\frac{-3}{2}}\Bigg(nK_{n-\frac{1}{2}}(k_1r_2)-k_1r_2K_{n+\frac{1}{2}}(k_1r_2)\Bigg)+C_n^{(2)}r_2^{\frac{-3}{2}}\Bigg(nK_{n-\frac{1}{2}}(k_2r_2)-k_2r_2K_{n+\frac{1}{2}}(k_2r_2)\Bigg)\Bigg]\Bigg|_{r_1=a_1}\frac{G_n(\zeta_2)}{\sqrt{1-\zeta_2^2}}=\frac{1}{\sqrt{1-\zeta_1^2}},\tag{4.11}$$

$$\sum_{n=2}^{\infty}\Bigg[(1-n)A_n^{(1)}r_1^{-n-1}+B_n^{(1)}a_1^{\frac{-3}{2}}\Bigg(nK_{n-\frac{1}{2}}(k_1r_1)-k_1r_1K_{n+\frac{1}{2}}(k_1r_1)\Bigg)+C_n^{(1)}a_1^{\frac{-3}{2}}\Bigg(nK_{n-\frac{1}{2}}(k_2r_1)-k_2r_1K_{n+\frac{1}{2}}(k_2r_1)\Bigg)\Bigg]\Bigg|_{r_2=a_2}\frac{G_n(\zeta_1)}{\sqrt{1-\zeta_1^2}},+\sum_{n=2}^{\infty}\Bigg[(1-n)A_n^{(2)}a_2^{-n-1}+B_n^{(2)}a_2^{\frac{-3}{2}}\Bigg(nK_{n-\frac{1}{2}}(k_1a_2)-k_1a_2K_{n+\frac{1}{2}}(k_1a_2)\Bigg)+C_n^{(2)}a_2^{\frac{-3}{2}}\Bigg(nK_{n-\frac{1}{2}}(k_2a_2),-k_2a_2K_{n+\frac{1}{2}}(k_2a_2)\Bigg)\Bigg]\frac{G_n(\zeta_2)}{\sqrt{1-\zeta_2^2}}=\frac{\bar{U}}{\sqrt{1-\zeta_2^2}},\tag{4.12}$$

$$\sum_{n=2}^{\infty}a_1^{\frac{-3}{2}}\Bigg[B_n^{(1)}k_1^2\Bigg((n-1)\xi^{-2}-\xi'^{-2})K_{n-\frac{1}{2}}(k_1a_1)-\xi^{-2}k_1a_1K_{n+\frac{1}{2}}(k_1a_1)\Bigg)+C_n^{(1)}k_2^2\Bigg((n-1)\xi^{-2}-\xi'^{-2})K_{n-\frac{1}{2}}(k_1a_1)-\xi^{-2}k_1a_1K_{n+\frac{1}{2}}(k_2a_1)\Bigg)\Bigg]\frac{G_n(\zeta_1)}{\sqrt{1-\zeta_1^2}}+\sum_{n=2}^{\infty}r_2^{\frac{-3}{2}}\Bigg[B_n^{(2)}k_1^2\Bigg((n-1)\xi^{-2}-\xi'^{-2})K_{n-\frac{1}{2}}(k_2r_2)-\xi^{-2}k_1r_2K_{n+\frac{1}{2}}(k_1r_2)\Bigg)+C_n^{(2)}k_2^2\Bigg((n-1)\xi^{-2}-\xi'^{-2})K_{n-\frac{1}{2}}(k_2r_2)-\xi^{-2}k_2r_2K_{n+\frac{1}{2}}(k_2r_2)\Bigg)\Bigg]\Bigg|_{r_1=a1}\frac{G_n(\zeta_2)}{\sqrt{1-\zeta_2^2}}=0,\tag{4.13}$$

$$\sum_{n=2}^{\infty}a_1^{\frac{-3}{2}}\Bigg[B_n^{(1)}k_1^2\Bigg((n-1)\xi^{-2}-\xi'^{-2})K_{n-\frac{1}{2}}(k_1r_1)-\xi^{-2}k_1r_1K_{n+\frac{1}{2}}(k_1r_1)\Bigg)+C_n^{(1)}k_2^2\Bigg((n-1)\xi^{-2}-\xi'^{-2})K_{n-\frac{1}{2}}(k_1r_1)-\xi^{-2}k_2r_1K_{n+\frac{1}{2}}(k_2r_1)\Bigg)\Bigg]\Bigg|_{r_2=a2}\frac{G_n(\zeta_1)}{\sqrt{1-\zeta_1^2}}+\sum_{n=2}^{\infty}a_2^{\frac{-3}{2}}\Bigg[B_n^{(2)}k_1^2\Bigg((n-1)\xi^{-2}-\xi'^{-2})K_{n-\frac{1}{2}}(k_2a_2)-\xi^{-2}k_1a_2K_{n+\frac{1}{2}}(k_1a_2)\Bigg)+C_n^{(2)}k_2^2\Bigg((n-1)\xi^{-2}-\xi'^{-2})K_{n-\frac{1}{2}}(k_2a_2)-\xi^{-2}k_2a_2K_{n+\frac{1}{2}}(k_2a_2)\Bigg)\Bigg]\frac{G_n(\zeta_2)}{\sqrt{1-\zeta_2^2}}=0.\tag{4.14}$$

This problem might be solved using the boundary collocation strategy established by Gluckman *et al.* [29]. But in order to do this, the complete infinite system of equations involving the unknown constants would need to be solved, which is not conceivable. Using the boundary colocation approach developed by Gluckman *et al.* [29], this challenge may be overcome. The steps involved in this technique are as follows: first, each infinite series must be truncated after a certain number $N \approx 60$ of terms in order for the number of unknown constants to become finite; next, a sufficient set of points on each spherical particle must be chosen as colocation points; at these points, boundary conditions must be applied in order to yield the same number of linear equations, $6N$ as those containing the unknown

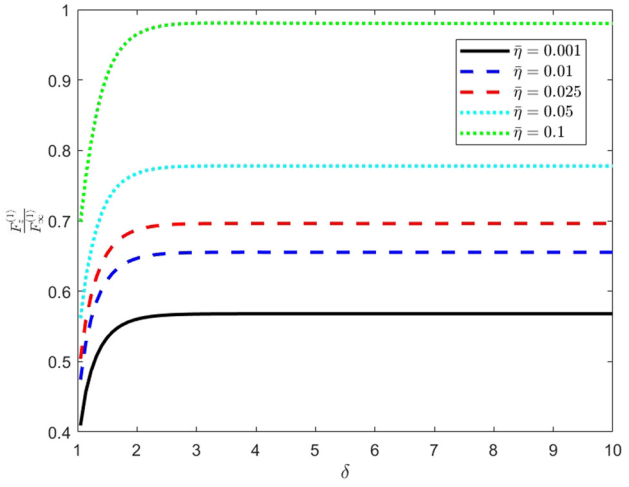

Figure 2: Drag force distribution versus the separation parameter δ for different first couple stress parameter $\bar{\eta}$ with the constant values of $\frac{U_2}{U_1} = 1.0$, $\frac{a_2}{a_1} = 1.0$, $\bar{\eta}' = 0.01$, and $R_H = 1.0$.

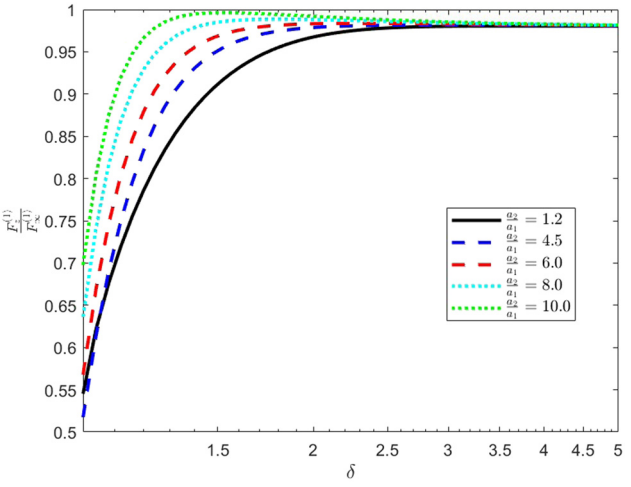

Figure 4: Drag force distribution versus the separation parameter δ for different size ratios $\frac{a_2}{a_1}$ with the constant values of $\frac{U_2}{U_1} = 1.0$, $\bar{\eta} = 0.1$, $\bar{\eta}' = 0.01$, and $R_H = 1.0$.

constants; and finally, the system of equations that results is solved to yield the unknown constants, allowing us to calculate the flow field. The hydrodynamic drag force $F_z^{(j)}$ with respect to $F_\infty^{(j)} = -6\mu\pi U_j a_j$ acting on the particle a_j may be obtained by using formula (3.6):

$$F_z^{(j)} = 2\mu\pi a^2 U_j a_j \left(\frac{2}{3} + A_2^{(j)}\right). \tag{4.15}$$

5 Numerical results

Non-Newtonian fluid flow has long been a topic of interest; many practicals have been conducted to expand the applications and advance contemporary technology. Scholars examined many forms of fluids and contributed to global modernization. One of the greatest subjects in fluid dynamics is couple stress fluids. Chemical engineering, manufacturing, polymer analysis, and biomedical engineering all make use of non-Newtonian fluids. This study shows the distributions of dimensionless drag force F_z/F_∞ versus the separation distance $\delta(=h/(a_1 + a_2))$ for unique values of couple stress parameters, η, η', the size ratio a_2/a_1, the velocity ratio U_2/U_1, the Hartmann number R_H, as shown in Figures 2–7 and Table 1. In addition, the streamlines in terms of the stream functions are displayed in Figures 8–12. The dimensionless Hartmann number

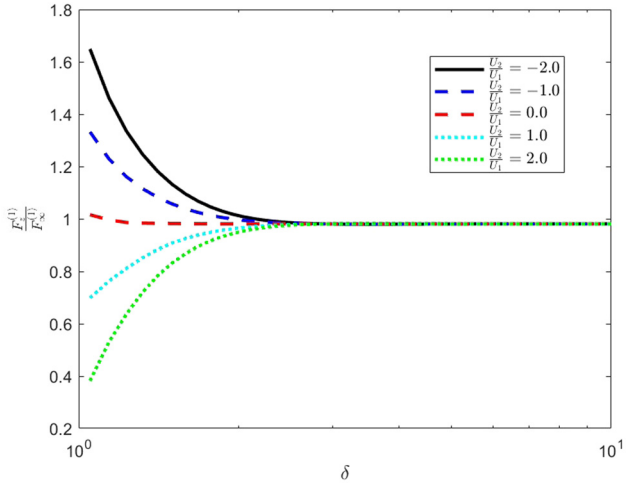

Figure 3: Drag force distribution versus the separation parameter δ for different velocities ratios $\frac{U_2}{U_1}$ with the constant values of $\frac{a_2}{a_1} = 1.0$, $\bar{\eta} = 0.1$, $\bar{\eta}' = 0.01$, and $R_H = 0.1$.

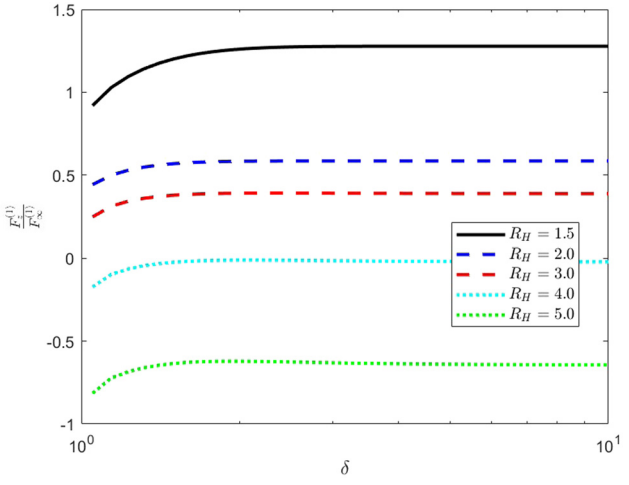

Figure 5: Drag force distribution versus the separation parameter δ for different Hartmann number RH with the constant values of $\frac{U_2}{U_1} = 1.0$, $\bar{\eta} = 0.001$, $\bar{\eta}' = 0.01$, $\frac{a_2}{a_1} = 1.0$.

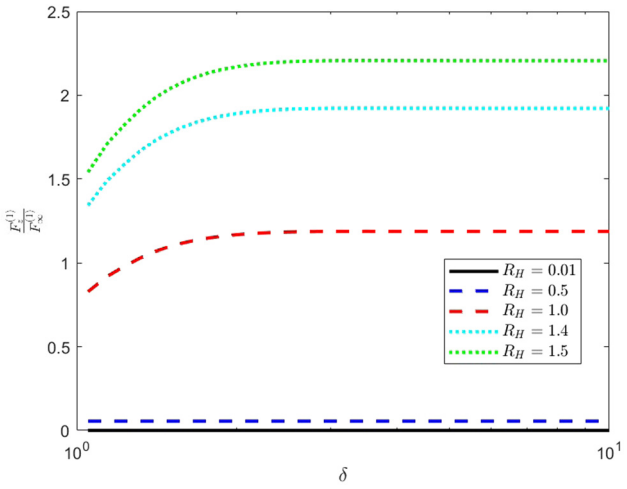

Figure 6: Drag force distribution versus the separation parameter δ for different Hartmann numbers with the constant values of $\frac{U_2}{U_1}$ = 1.0, $\bar{\eta}$ = 0.1, $\bar{\eta}'$ = 0.01, and $\frac{a_2}{a_1}$ = 1.0.

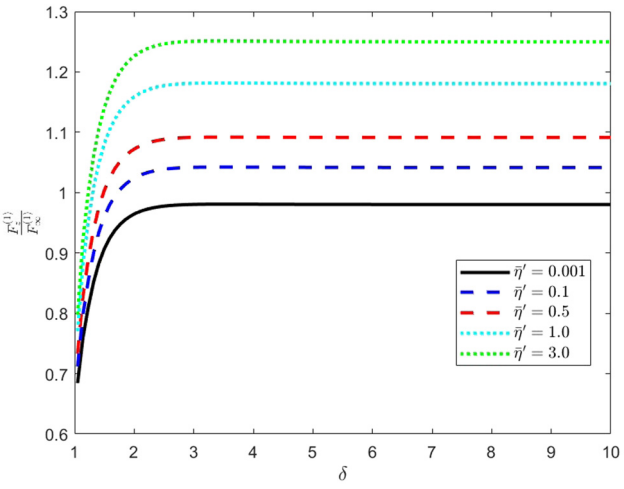

Figure 7: Drag force distribution versus the separation parameter δ for different $\bar{\eta}'$ with the constant values of $\frac{U_2}{U_1}$ = 1.0, $\bar{\eta}$ = 0.1, $\frac{a_2}{a_1}$ = 1.0, and R_H = 1.0.

measures the relative significance of magnetic induction drag and viscous drag. Furthermore, the electric and magnetic fields have many applications. Given that blood is a fluid that conducts electricity and the Lorentz force opposes the motion of conducting fluids according to Lenz's law, the principles of MHD therapy can be used to slow the flow of blood through the human artery system, which can help treat certain cardiovascular disorders.

- Figure 2 represents the separation distance for different first couple stress parameters, versus the normalized drag force. It is observed that the drag force, increases gradually with both the increase of separation distance

Table 1: Dimensionless drag force on the rigid sphere a_1 for different relevant factors with $\bar{\eta}'$ = 0.01 and the two equal spheres

		F_z/F_0					
		R_H = 0.0 (Ref [4])			R_H = 1.0		
$\frac{U_2}{U_1}$	δ	$\bar{\eta}$ = 0.001	$\bar{\eta}$ = 0.025	$\bar{\eta}$ = 0.1	$\bar{\eta}$ = 0.001	$\bar{\eta}$ = 0.025	$\bar{\eta}$ = 0.1
	1.05	0.942388	0.961502	1.007459	0.423299	0.481470	0.705180
	2.0	0.989002	1.009977	1.056119	0.580938	0.666808	1.023915
	3.0	1.000166	1.022736	1.072481	0.588492	0.675521	1.041810
1.0	4.0	1.003849	1.027253	1.078907	0.588908	0.675904	1.042120
	5.0	1.005496	1.029437	1.082338	0.588919	0.675875	1.041809
	6.0	1.006375	1.030693	1.084480	0.588925	0.675866	1.041677
	7.0	1.006902	1.031500	1.085948	0.588935	0.675872	1.041634
	8.0	1.007244	1.032059	1.087020	0.588946	0.675881	1.041624
	9.0	1.007481	1.032468	1.087837	0.588954	0.675889	1.041625
	10.0	1.007653	1.032780	1.088482	0.588961	0.675896	1.041629
	1.05	1.130650	1.185593	1.315125	0.745426	0.859470	1.393453
	2.0	1.034587	1.070941	1.153892	0.597014	0.684985	1.059540
	3.0	1.019071	1.051395	1.124588	0.589474	0.676317	1.041456
1.0	4.0	1.014251	1.044880	1.113957	0.589064	0.675947	1.041205
	5.0	1.012174	1.041874	1.108691	0.589054	0.675977	1.041523
	6.0	1.011095	1.040207	1.105593	0.589048	0.675986	1.041657
	7.0	1.010460	1.039167	1.103566	0.589037	0.675980	1.041700
	8.0	1.010054	1.038463	1.102141	0.589027	0.675971	1.041709
	9.0	1.009777	1.037960	1.101085	0.589018	0.675962	1.041708
	10.0	1.009578	1.037583	1.100272	0.589012	0.675955	1.041704

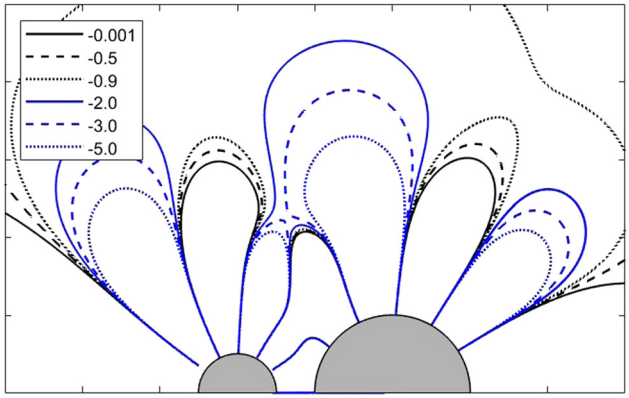

Figure 8: Streamlines for certain values of $\bar{\eta}' = 0.01$, $\frac{U_2}{U_1} = 1.0$, $\bar{\eta} = 0.001$, $\frac{a_2}{a_1} = 1.0$, $R_H = 1.0$, and $\delta = 1.05$.

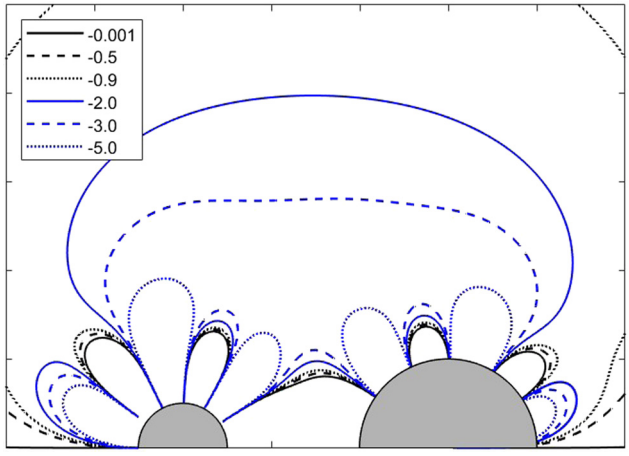

Figure 9: Streamlines for certain values of $\bar{\eta}' = 0.01$, $\frac{U_2}{U_1} = 1.0$, $\bar{\eta} = 0.001$, $\frac{a_2}{a_1} = 1.0$, $R_H = 1.0$, and $\delta = 3.0$.

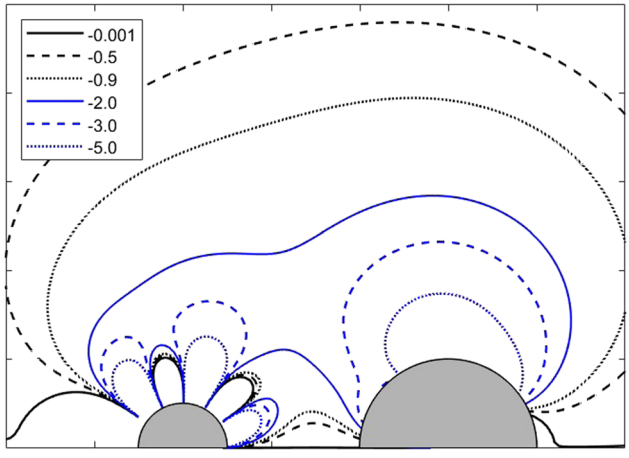

Figure 10: Streamlines for certain values of $\bar{\eta}' = 0.01$, $\frac{U_2}{U_1} = 2.0$, $\bar{\eta} = 0.001$, $\frac{a_2}{a_1} = 1.0$, $R_H = 2.0$, and $\delta = 3.0$.

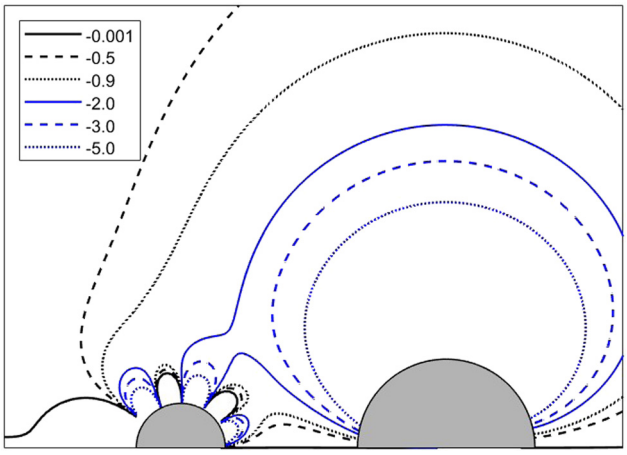

Figure 11: Streamlines for certain values of $\bar{\eta}' = 0.01$, $\frac{U_2}{U_1} = 2.0$, $\bar{\eta} = 0.01$, $\frac{a_2}{a_1} = 2.0$, $R_H = 2.0$, and $\delta = 3.0$.

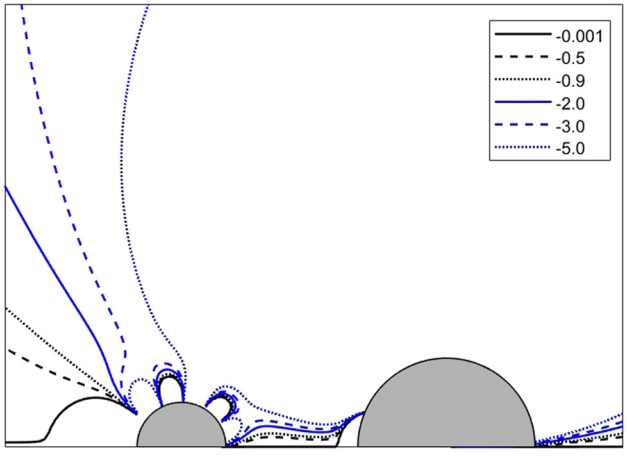

Figure 12: Streamlines for certain values of $\bar{\eta}' = 0.01$, $\frac{U_2}{U_1} = 4.0$, $\bar{\eta} = 0.1$, $\frac{a_2}{a_1} = 4.0$, $R_H = 1.0$, and $\delta = 3.0$.

and the first couple stress parameters, which physically coincide with the fact that states when the sphere translates alone in the absence of the second force, it has a significant force at the two spheres moving in the same direction with the same velocities and equal in size with certain values of $R_H = 1.0$, $\bar{\eta}' = 0.01$.

- In Figure 3, the normalized drag force is plotted against the separation distance for different velocity ratio parameters. It has been observed that drag force increases gradually as separation distance increases and decreases as the velocity ratio increases. Physically, drag opposes object motion just like friction does. In this case, two solid spheres have the same size with equal speeds at $R_H = 1.0$, $\bar{\eta}' = 0.01$, and $\bar{\eta} = 0.1$.
- Figure 4 illustrates the normalized drag force corresponding to the separation distance for different size

ratio parameters. It has been observed that when the sphere $a_2 = 10a_1$ the drag force tends to unity and also it increases with both the separation distance and the size ratio. Physically, drag opposes object motion just like friction does. In this case, the two solid spheres move in the same direction with the same speeds with the other certain values being $R_H = 1.0$, $\bar{\eta}' = 0.01$, and $\bar{\eta} = 0.1$.
- Figures 5 and 6 display the normalized drag force corresponding to the separation distance for different Hartmann numbers. For high values $f\ R_H$, the normalized drag force inclines with the increase of R_H at $\bar{\eta} = 0.001$ but for small values of R_H at $\bar{\eta} = 0.1$, the normalized drag force increases with the increase of R_H with the other certain values being $U_2/U_1 = 1.0$, $\bar{\eta}' = 0.01$, and $a_2/a_1 = 1.0$.
- Figure 7 shows the normalized drag force corresponding to the separation distance for different second couple stress fluid parameters. It seems that the improvement of the normalized drag force improves with the increase of $\bar{\eta}'$ with the other certain values being $U_2/U_1 = 1.0$, $\bar{\eta} = 0.1$, $a_2/a_1 = 1.0$, $R_H = 1.0$.
- Figures 8–12 depict the streamlines of the constant stream function with the other constant values of the parameters U_2/U_1, $\bar{\eta}$, $\bar{\eta}'$, a_2/a_1, R_H, and δ.

6 Conclusions

This article examines the migration of two rigid objects moving in a straight line through an incompressible fluid with couple stress properties. The migration is analyzed in terms of its progression and uniformity, specifically under the influence of a magnetic field. The concept of superposition is used to generate an infinite series, which serves as the general solution for the continuous translational movements of a couple stress fluid traveling through an axisymmetric structure. Using this method to build two spherical coordinate frames with origins at the centers of the two spherical particles solves the problem. Using the boundary collocation approach to limit the spherical bounds, we may find the unknown constants in the truncated series. We provide and display the numerical results of the normalized drag applied to an object. These findings demonstrated how quickly the numerical values converge to at least six decimal places. The normalized force of drag is significantly influenced by the physical parameters δ, U_2/U_1, a_2/a_1, $\bar{\eta}$, $\bar{\eta}'$, and R_H. The key observations and the numerical findings of the current study can be summarized as follows:
- The impact of R_H with $\bar{\eta}$ on the normalized force of drag on each of the sphere is more significant.
- It is detected that the drag force generally rises as the couple stress parameters rise and falls as the Hartmann number rises. This is because permitting the microelements to generate less overall proportionate motion between the fluid and the particle minimizes the drag force.
- At significantly higher-frequency parameters, the velocity is noted to approach zero at the center of the microannulus.
- To further comprehend the behavior of fluid flow when the magnetic field strength is raised, streamlines are displayed.
- Finally, by setting the viscosity coefficient to zero and $R_H = 0$, the specific case of binary translating spheres in a viscous fluid is generated.

This study holds numerous applications in fluid dynamics and couple stress fluids are one of the trendiest subjects. Non-Newtonian fluids have applications in polymer analysis, manufacturing, chemical engineering, and biomedical engineering.

Funding information: This research was supported by Princess Nourah bint Abdulrahman University Researchers Supporting Project Number (PNURSP2024R522), Princess Nourah Bint Abdulrahman University, Riyadh, Saudi Arabia.

Author contributions: All authors were involved in the overall planning and design of the study. Shreen El-Sapa was responsible for gathering materials, collecting data, and analyzing the results. Munirah Aali Alotaibi wrote the initial draft of the manuscript, which was then reviewed and improved upon by all authors. All authors have accepted responsibility for the entire content of this manuscript and approved its submission.

Conflict of interest: The authors state no conflict of interest.

Data availability statement: All data generated or analysed during this study are included in this published article.

References

[1] Bearman PW, Wadcock AJ. The interaction between a pair of circular cylinders normal to a stream. J Fluid Mechanics. 1973;61(3):499–511.
[2] Yutaka T, Morikawa Y, Terashima K. Fluid-dynamic interaction between two spheres. Int J Multiphase Flow. 1982;8(1):71–82.
[3] Faltas MS, Sherief HH, Ashmawy EA. Interaction of two spherical particles rotating in a micropolar fluid. Math Comput Model. 2012;56(9-10):229–39.
[4] Shehadeh TH, Ashmawy EA. Interaction of two rigid spheres translating collinearly in a couple stress fluid. Europ J Mechanics-B/Fluids 2019;78:284–90.
[5] Chandrasekhar S. The stability of viscous flow between rotating cylinders in the presence of a magnetic field. Proc R Soc London Ser A Math Phys Sci 1953;216(1126):293–309.

[6] Davis RH, Jean-Marc S, Hinch EJ. The elastohydrodynamic collision of two spheres. J Fluid Mechanics 1986;163:479–97.
[7] Stewartson K. Motion of a sphere through a conducting fluid in the presence of a strong magnetic field. Mathematical Proceedings of the Cambridge Philosophical Society. Vol. 52. No. 2. Cambridge University Press, 1956.
[8] Saad EI. Effect of magnetic fields on the motion of porous particles for Happel and Kuwabara models. J Porous Media. 2018;21(7):637–664.
[9] Srivastava BG. Hydrodynamic permeability of a membrane composed of porous spherical particles in the presence of uniform magnetic field. Colloid J. 2014;76:725–38.
[10] Madasu KP, Bucha T. Steady viscous flow around a permeable spheroidal particle. Int J Appl Comput Math. 2019;5:1–13.
[11] Madasu KP, Bucha T. Impact of magnetic field on flow past cylindrical shell using cell model. J Brazilian Soc Mech Sci Eng. 2019;41(8):320.
[12] El-Sapa S. The force on a magneto-spherical particle oscillating in a viscous fluid perpendicular to an impermeable planar wall with slippage. Europ J Pure Appl Math. 2022;15(3):1376–401.
[13] El-Sapa S, Alsudais NS. Effect of magnetic field on the motion of two rigid spheres embedded in porous media with slip surfaces. Europ Phys J E 2021;44(5):68.
[14] El-Sapa S, Faltas MS. Mobilities of two spherical particles immersed in a magneto-micropolar fluid. Phys Fluids 2022;34(1):013104.
[15] Raza J, Mebarek-Oudina F, Chamkha AJ. Magnetohydrodynamic flow of molybdenum disulfide nanofluid in a channel with shape effects. Multidiscipline Model Materials Struct. 2019;15(4):737–57.
[16] Veera KM, Chamkha AJ. Hall and ion slip effects on MHD rotating flow of elastico-viscous fluid through porous medium. Int Commun Heat Mass Transfer. 2020;113:104494.
[17] Kashyap KP, Ojjela O, Das SK. Magnetohydrodynamic mixed convective flow of an upper convected Maxwell fluid through variably permeable dilating channel with Soret effect. Pramana. 2019;92:1–10.
[18] Singh JK, Joshi N, Begum SG. Unsteady magnetohydrodynamic Couette-Poiseuille flow within porous plates filled with porous medium in the presence of a moving magnetic field with Hall and ion-slip effects. Int J Heat Technol. 2016;34(1):89–97.
[19] Sakthikala R, Lavanya V. MHD rotating flow through a porous medium embedded in a second grade fluid. Nveo-Natural Volatiles Essential Oils J | Nveo 2021;8:1730–46.
[20] Nadeem S, Akram S. Peristaltic flow of a couple stress fluid under the effect of induced magnetic field in an asymmetric channel. Archive Appl Mechanics. 2011;81:97–109.
[21] Hassan AR. The entropy generation analysis of a reactive hydromagnetic couple stress fluid flow through a saturated porous channel. Appl Math Comput. 2020;369:124843.
[22] Srinivasacharya D, Madhava Rao G. MHD effect on the couple stress fluid flow through a bifurcated artery. Proc Eng. 2015;127:877–84.
[23] Ali N, Khan SU, Muhammad S, Zaheer S, Abbas A. MHD flow and heat transfer of couple stress fluid over an oscillatory stretching sheet with heat source/sink in porous medium. Alexandria Eng J. 2016;55(2):915–24.
[24] Aali Alotaibi M, El-Sapa S. MHD couple stress fluid between two concentric spheres with slip regime. Results Eng 2024;21:101934.
[25] Hoffmann K, Marx D, Botkin ND. Drag on spheres in micropolar fluids with non-zero boundary conditions for microrotations. J Fluid Mechanics. 2007;590:319–30.
[26] Ashmawy EA. A general formula for the drag on a sphere placed in a creeping unsteady micropolar fluid flow. Meccanica. 2012;47(8):1903–12.
[27] Shu J, Lee JS. Fundamental solutions for micropolar fluids. J Eng Math. 2008;61:69–79.
[28] Sherief HH, Faltas MS, El-Sapa S. A general formula for the drag on a solid of revolution body at low Reynolds numbers in a microstretch fluid. Meccanica. 2017;52:2655–64.
[29] Gluckman MJ, Pfeffer R, Weinbaum S. A new technique for treating multiparticle slow viscous flow: axisymmetric flow past spheres and spheroids. J Fluid Mechanics. 1971;50(4):705–40.
[30] Sherief HH, Faltas MS, El-Sapa S. Force on a spherical particle oscillating in a viscous fluid perpendicular to an impermeable planar wall. J Brazilian Soc Mech Sci Eng. 2019;41(6):244.
[31] Sherief HH, Faltas MS, El-Sapa S. Axisymmetric creeping motion caused by a spherical particle in a micropolar fluid within a nonconcentric spherical cavity. Europ J Mechanics-B/Fluids. 2019;77:211–20.
[32] Kolodziej JA. View Kolodziej of application of boundary collocation methods in mechanics of continuous media. SM Archives. 1987;12(4):187–231.
[33] Al-Hanaya A, El-Sapa S, Ashmawy EA. Axisymmetric motion of an incompressible couple stress fluid between two eccentric rotating spheres. J Appl Mech Tech Phys. 2022;63(5):790–8.
[34] Alsudais NS, El-Sapa S, Ashmawy EA. Stokes flow of an incompressible couple stress fluid confined between two eccentric spheres. Europ J Mechanics-B/Fluids. 2022;91:244–52.
[35] El-Sapa S, Almoneef AA. The axisymmetric migration of an aerosol particle embedded in a Brinkmann medium of a couple stress fluid with slip regime. Europ J Pure Appl Math. 2022;15(4):1566–92.
[36] Abbas AA. Generalized thermoelastic interaction in functional graded material with fractional order three-phase lag heat transfer. J Cent South Univ. 2015;22:1606–13. doi: 10.1007/s11771-015-2677-5.
[37] Saeed T, Abbas IA. Finite element analyses of nonlinear DPL bioheat model in spherical tissues using experimental data. Mech Based Des Struct Mach. 2020;50:1287–97. doi: 10.1080/15397734.2020.1749068.
[38] Abbas I, Hobiny A, Alshehri H, Vlase S, Marin M. Analysis of thermoelastic interaction in a polymeric orthotropic medium using the finite element method. Polymers (Basel). 2022;14:2112. doi: 10.3390/polym14102112.
[39] Abb Haider J, Ahmad S, Ghazwani HA, Hussien M, Almusawa MY, Az-Zo'bi EA. Results validation by using finite volume method for the blood flow with magnetohydrodynamics and hybrid nanofluids. Modern Phys Lett BVol. 2024;38(24):2450208.
[40] Muhammad K, Ahmed B, Sharaf M, Afikuzzamand M, Az-Zo'bie EA. Multiscale tribology analysis of MHD hybrid nanofluid flow over a curved stretching surface. Nanoscale Adv. 2024;6:855.
[41] Khan MN, Khan AA, Alqahtani AM, Wang Z, Hejazi HA, Az-Zo'bi EA. Chemically reactive aspects of stagnation-point boundary layer flow of second-grade nanofluid over an exponentially stretching surface. Numer Heat Transfer B Fundamentals. doi: 10.1080/10407790.2024.2318456.
[42] Stokes VK. Couple stresses in fluids. Theories of fluids with microstructure: an introduction. 1984. p. 34–80.
[43] Prasad MK, Sarkar P. Slow flow past a slip sphere in cell model: magnetic effect. Recent trends in fluid dynamics research: select proceedings of RTFDR 2021. Singapore: Springer; 2022.
[44] Happel J, Brenner H. Low Reynolds number hydrodynamics: with special applications to particulate media. Springer Science and Business Media. Vol. 1. 1983.
[45] Prasad MK, Sarkar P. An analytical study of couple stress fluid through a sphere with an influence of the magnetic field. J Appl Math Comput Mechanics. 2022;21(3):99–110.